

# **Title:**

**Molecular features similarities between SARS-CoV-2, SARS, MERS and key human genes could favour the viral infections and trigger collateral effects.**

**Authors:** Lucas L. Maldonado<sup>1</sup> and Laura Kamenetzky<sup>1</sup>

**Affiliations:** <sup>1</sup>IMPAM, CONICET, Facultad de Medicina, Universidad de Buenos Aires, Ciudad Autónoma de Buenos Aires, Argentina. <sup>2</sup>

**e-mails:** lucas.l.maldonado@gmail.com; lkamenetzky@fmed.uba.ar

## **Abstract**

In December 2019 rising pneumonia cases caused by a novel  $\beta$ -coronavirus (SARS-CoV-2) occurred in Wuhan, China, which has rapidly spread worldwide causing thousands of deaths. The WHO declared the SARS-CoV-2 outbreak as a public health emergency of international concern therefore several scientists are dedicated to the study of the new virus. Since human viruses have codon usage biases that match highly expressed proteins in the tissues they infect and depend on host cell machinery for replication and co-evolution, we selected the genes that are highly expressed in the tissue of human lungs to perform computational studies that permit to compare their molecular features with SARS, SARS-CoV-2 and MERS genes. In our studies, we analysed 91 molecular features for 339 viral genes and 463 human genes that consisted of 677873 codon positions. Hereby, we found that A/T bias in viral genes could propitiate the viral infection favoured by a host dependant specialization using the host cell machinery of only some genes. The envelope protein E, the membrane glycoprotein M and ORF7 could have been further benefited by a high rate of A/T in the third codon position. Thereby, the mistranslation or de-regulation of protein synthesis could produce collateral effects, as a consequence of viral occupancy of the host translation machinery due to molecular similarities with viral genes. Furthermore, we provided a list of candidate human genes whose molecular features match those of SARS-CoV-2, SARS and MERS genes, which should be considered to be incorporated into genetic population studies to evaluate the susceptibility to respiratory viral infections caused by these viruses. The results presented here, settle the basis for further research in the field of human genetics associated with the new viral infection, COVID-19, caused by SARS-CoV-2 and for the development of antiviral preventive methods.

## 33 **Keywords**

34 SARS-CoV-2, SARS, MERS, codon usage, viral genes, human infection, COVID-19

## 35 **1. Introduction**

36 Since its initial outbreak at Huanan Seafood Wholesale Market in Wuhan, China, in late  
 37 2019, COVID-19 has affected more than 4 million people and caused more than 300  
 38 thousand deaths all around the world. Thereafter, scientists are focused not only on  
 39 studying the biology and dissemination of COVID-19 to control the transmission and  
 40 design proper diagnostic tools and treatments, but also they are racing to design a  
 41 vaccine that could prevent the infection caused by the coronavirus SARS-CoV-2. This  
 42 virus belongs to the Betacoronavirus ( $\beta$ -coronavirus) of the *Coronaviridae* family, which  
 43 is also composed of three more genera:  
 44 Alphacoronavirus ( $\alpha$ CoV), Gammacoronavirus ( $\gamma$ CoV) and Deltacoronavirus ( $\delta$ CoV)  
 45 (Chen et al., 2020a). Viruses from this family possess a single-stranded, positive-sense  
 46 RNA and the genome ranges from 26 to 32 kb (Su et al., 2016).

47 Coronaviruses have been identified in several host species including humans, bats,  
 48 civets, mice, dogs, cats, cows and camels (Cavanagh, 2007; Clark, 1993; Wang et al.,  
 49 2006; Zhou et al., 2018). Since severe acute respiratory syndrome (SARS), caused by  
 50 the coronavirus SARS-CoV, emerged in southern China in 2002 (Peiris et al., 2004),  
 51 several studies tracing the transmission and possible reservoirs for viruses have been  
 52 performed. In early 2007, it had already been warned that bats were a natural reservoir  
 53 for an increasing number of emerging zoonotic viruses as well as for a large number of  
 54 viruses that have a close genetic relationship with the coronaviruses that cause the severe  
 55 acute respiratory syndrome. Furthermore, it was warned that these viruses possess more  
 56 risk than other pathogens for disease emergence in human and domestic mammals  
 57 because of their higher mutation rates (Wang et al., 2006). Moreover, legal and illegal  
 58 trading of wildlife animals propitiates the environment for cross-species virus  
 59 transmission contributing to the rapid spread of the viral infections around the  
 60 world (Wang et al., 2006; Wong et al., 2019) as already occurred with SARS and the  
 61 Middle East respiratory syndrome (MERS) (Zaki et al., 2012). Both viruses have likely  
 62 originated in bats and are genetically diverse coronaviruses (Cui et al., 2019). Currently,  
 63 the outbreak of an atypical pneumonia caused by the novel coronavirus SARS-CoV-2  
 64 appears to have also started from a zoonotic and a cross-species virus transmission at a

market in Wuhan including bats and pangolins, where animals were kept together and the meat was sold (Chan et al., 2020).

Due to viruses replicate exclusively inside of living cells and depend exclusively on the protein synthesis and chaperones machinery of their host, we speculated that the primary structure of viral genes might be determined by the same forces that shape the codon usage in the hosts' genes. Thereby, viral molecular patterns and codon usage preferences would be a reflection of the host machinery. Codon pair bias and dinucleotide preferences of viruses have been suggested as the main factors that reflect the codon usage of their hosts. Indeed, virus attenuation by codon pair deoptimization is used as an efficacious attenuation method of various small RNA viruses and has resulted in the generation of superior experimental live virus vaccines (Coleman et al., 2008; Mueller et al., 2010; Nouën et al., 2014; Shen et al., 2015; Wang et al., 2015; Yang et al., 2013).

In order to contribute to solving the sanitary emergence, here we provide a thorough and comprehensive analysis that could help to understand the viability of the virus as well as the susceptibility of the human host to the viral infection based on the molecular patterns of their genes. Therefore, the main goals of our work were to study the molecular and evolutionary aspects of the human coronaviruses SARS-CoV-2, SARS and MERS and to determine the level of similarity of the codon usage and molecular features between the genes of human coronaviruses and the human genes in order to identify the factors that are responsible for the codons selection in the viruses. Moreover, we proposed to identify the essential viral genes for viral replication and human genes whose translation machinery is involved in propitiating the system for viral replication in order to determine whether the genetic population variability could be involved in modelling the gene features and therefore contributing to the human susceptibility to viral infections.

## 2. Methods

Up to late April, a total of ~500 SARS-CoV-2  $\beta$ -coronavirus genome became available. The total available sequences of  $\beta$ -coronavirus were downloaded from the NCBI (<https://www.ncbi.nlm.nih.gov/labs/virus/vssi/#/>) including the reference genomes of MERS (NC\_019843), SARS (NC\_004718) and SARS-CoV-2 (NC\_045512) and were classified according to their host. Different SARS-CoV-2 isolates from different countries were pre-analysed but only reference genomes were retained due to the low

variability of the data. The genomes quality was assessed and the genomes containing more than 10 gaps were discarded. CDS of representative viruses from the previous classification were selected and analysed. Since human viruses have codon usage biases (CUB) that match highly expressed proteins in the tissues they infect (Miller et al., 2017) we selected 463 highly expressed human genes in lung tissues according to the fold-change between the expression level in lung and the tissue with second-highest expression level according to the “Human Protein Atlas” (<https://www.proteinatlas.org/humanproteome/tissue/lung>). We considered valid CDS when they started with an ATG codon, ended with an in-frame stop codon, and had no undetermined nucleotides nor internal stop codons. The accession numbers of the sequences that were used here can be found in Supplementary file 1.

The CUB analyses were performed with CodonW 1.4.4 (J Peden, <http://codonw.sourceforge.net/>). The total GC content of the CDS as well as the GC content of the first (P1), second (P2), and third (P3) codon positions were calculated using custom PERL scripts. To correct the inequality composition at the third codon position (Sueoka, 1988), the three stop codons (UAA, UAG, and UGA) were excluded in the calculation of P3, and the two single codons for methionine (AUG) and tryptophan (UGG) were excluded from P1, P2, and P3.

## 2.1. Codon usage indices

The following codon indices were calculated: relative synonymous codon usage (RSCU) (Sharp and Li, 1987), the effective number of codons (ENc) (Wright, 1990), codon adaptation index (CAI) (Lee et al., 2010; Sharp and Li, 1987), codon bias index (CBI) (Bennetzen and Hall, 1982), the optimal frequency of codons (Fop) (Ikemura, 1981), General Average Hydropathicity (GRAVY) (Sharp and Li, 1987), aromaticity (Aromo) (Lobry and Gautier, 1994) and GC-content at the first, second and third codon positions (GC1, GC2 and GC3), frequency of either a G or C at the third codon position of synonymous codons (GC3s), the average of GC1 and GC2 (GC12) and Translational selection (TrS2).

ENc indicates the degree of codon bias for individual genes. Over a range of values from 20 to 61, lower values indicate higher codon bias, while ENc equal to 61 means that all codons are used with equal probability (Novembre, 2002; Wright, 1990).

CAI values measure the extent of bias toward preferred codons in highly expressed genes. CAI values range between 0 and 1.0, with higher CAI values

131 indicating higher expression and higher CUB (Lee et al., 2010; Sharp and Li, 1987)  
 132 under the assumption that translational selection would optimize gene sequences  
 133 according to their expression levels.

134 CBI is another measure of directional codon bias, based on the degree of  
 135 preferred codons used in a gene, like to the frequency of optimal codons. It measures  
 136 the extent to which a gene uses a subset of optimal codons. In genes with extreme codon  
 137 bias, CBI will be equal to 1, whereas in genes with random codon usage the CBI values  
 138 will be equal to 0 (Bennetzen and Hall, 1982).

139 Fop is a species-specific measure of bias towards particular codons that appear  
 140 to be translationally optimal in particular species. It can be calculated as the ratio  
 141 between the frequency of optimal codons and the total number of synonymous codons.  
 142 Its values range from 0 if a gene contains no optimal codons to 1 if a gene is entirely  
 143 composed of optimal codons (Ikemura, 1981). The determination of optimal codons was  
 144 carried out based on the axis 1 ordination, the top and bottom 5% of genes were  
 145 regarded as the high and low bias datasets, respectively. Codon usage in the two data  
 146 sets was compared using chi-square tests, with the sequential Bonferroni correction to  
 147 assess significance according to Peden (Peden, 1999). Optimal codons were defined as  
 148 those that are used at significantly higher frequencies ( $p$ -value  $< 0.01$ ) in highly  
 149 expressed genes compared with the frequencies in genes expressed at low levels.

150 GRAVY values were calculated as a sum of the hydropathy values of all the  
 151 amino acids encoded by the codons in the gene product divided by the total number of  
 152 residues in the sequence of the protein. The more negative the GRAVY value, the more  
 153 hydrophilic the protein is, whereas while the more positive the GRAVY value, the more  
 154 hydrophobic the protein (Sharp and Li, 1987).

155 Aromo values denote the frequency of aromatic amino acids (Phe, Tyr, Trp)  
 156 encoded by the codons in the gene product. (Lobry and Gautier, 1994).

157 TrS2 estimates the codon-anticodon interaction efficiency revealing bias in  
 158 favour of optimal codon-anticodon energy and represents the translational efficiency of  
 159 a gene. TrS2 value  $> 0.5$  shows bias in favour of translational selection according to  
 160 Gouy and Gautier (Gouy and Gautier, 1982; Uddin et al., 2017; Uddin and Chakraborty,  
 161 2018).

## 162 **2.2. Codon Pair Score and Codon Pair Bias**

163 The determination of codon pair biases in coding sequences was performed

164 using CPBias (<https://rdrr.io/github/alex-sbu/CPBias/>) developed in R. as described by  
 165 Coleman et al.(Coleman et al., 2008). The CPS is defined as the natural logarithm of the  
 166 ratio of the observed over the expected number of occurrences of a particular codon pair  
 167 in all protein-coding sequences of a species. The CPB was used as an index and also to  
 168 determine the bias in CPS among the virus and host genes. The expected number of  
 169 codon pair occurrences estimates the number of codon pairs to be present if there is no  
 170 association between the codons that form the codon pair. It is also calculated to be  
 171 independent of codon bias and amino acid frequency (Coleman et al., 2008). A negative  
 172 CPS value means that a particular codon pair is underrepresented, whereas a positive  
 173 CPS value indicates that a particular codon pair is overrepresented in the analysed  
 174 protein-coding sequences. Codon pairs that are equally under- or overrepresented have a  
 175 CPS equidistant from 0. We calculated CPS for each of the 3,721 possible codon pairs  
 176 (61 x 61 codons).

### 177 **2.3. ENc-plots**

178 The ENc-plot was used to analyse the influence of base the composition on the  
 179 codon usage in a genome (Hartl et al., 1994). The ENc values were plotted against  
 180 GC3s values and a standard curve was generated to show the functional relationship  
 181 between ENc and GC3s values under mutational bias rather than selection pressure. In  
 182 genes where codon choice is constrained only by a G+C mutational bias, the predicted  
 183 ENc values will lie on or close to the GC3s standard curve. However, the presence of  
 184 other factors, such as selection effects, causes the values to deviate considerably from  
 185 the expected GC3s curve. The values of ENc range from 20 (when only one codon is  
 186 used per amino acid) to 61 (when all codons are used with equal probability). The  
 187 predicted values of ENc were calculated according to Hartl *et al.*(Hartl et al., 1994).

### 188 **2.4. Clustering analysis**

189 A total of 91 variables of codon usage of viruses and human genes, including the  
 190 gene composition, RSCU frequencies and the indices described in M&M section,were  
 191 integrated into an input matrix to feed the clustering algorithm. The analysed variables  
 192 can be found in supplementary file 1. Hierarchical clustering using Euclidean distances  
 193 was performed. clValid package clustering algorithm was used to choose and validate  
 194 the best clustering method. Flexible Procedures for Clustering (fpc:[https://cran.r-](https://cran.r-project.org/web/packages/fpc/index.html)  
 195 [project.org/web/packages/fpc/index.html](https://cran.r-project.org/web/packages/fpc/index.html)) was used for bootstrapping (n=100) and

196 evaluate the cluster stability. Clustering method was used to establish genes groups  
197 from codon usage similarities among virus and human genes.

## 198 **2.5. Principal component analysis (PCA)**

199 Principal component analysis (PCA) was used to evaluate the codon usage  
200 variation among genes as the multivariate statistical method. The axes represent and  
201 allow to identify the most prominent factors contributing to the variation among the  
202 genes. Since there are a total of 59 synonymous codons (including 61 sense codons,  
203 minus the unique Met and Trp and stop codons), the degrees of freedom were reduced to  
204 40 at removing variations caused by the unequal usage of amino acids during the  
205 correspondence analysis of RSCU (Greenacre, 1984). The data were normalized  
206 according to Sharp and Li (Sharp and Li, 1987) in order to define the relative  
207 adaptiveness of each codon (Peden, 1999; Suzuki et al., 2005), codon usage indices  
208 described above were also included as variables. PCA analyses were performed using  
209 “factoextra R package” ([https://cloud.r-](https://cloud.r-project.org/web/packages/factoextra/index.html)  
210 [project.org/web/packages/factoextra/index.html](https://cloud.r-project.org/web/packages/factoextra/index.html)).

## 211 **2.6. Phylogenetic analyses**

212 The DNA genome sequences of all the viruses were aligned using ClustalO  
213 v1.2.4 (Sievers et al., 2011). PartitionFinder 2 (Lanfear et al., 2016) was used to select  
214 the best-fit partitioning schemes and models of evolution for the phylogenetic  
215 analysis. The evolutionary model was set on generalised time-reversible substitution  
216 model with gamma-distributed rate variation across the sites and a proportion of  
217 invariable sites (GTR +G). The final phylogeny was calculated using fasttree (Price et  
218 al., 2009). The bootstrap consensus trees inferred from 1000 replicates were retained in  
219 the bootstrap and the final trees were drawn using Figtree  
220 (<https://github.com/rambaut/figtree/releases>).

## 221 **3. Results**

### 222 **3.1. Phylogeny**

223 Up to late April, a total of  $\approx$  500 SARS-CoV-2  $\beta$ -coronavirus genomes became  
224 available and the number of available genomes incremented substantially. The total  
225 available sequences of  $\beta$ -coronavirus were downloaded from the NCBI. In order to  
226 evaluate the variability and to select the best candidates for codon usage and nucleotides



content analyses, we performed phylogenetic analyses by implementing the GTR + G model according to partition finder results. Firstly, a phylogenetic tree was constructed (data not shown) using the whole genome sequences of SARS-CoV-2 reported in humans from Spain, USA, Italy, South America, China, Korea Japan and Australia, the references genomes of MERS and SARS and the viruses genomes isolated from bats, pangolins, civets, hedgehogs, *Bos taurus*, and canids (Supplementary file 1). Since all SARS-CoV-2 genome sequences remained together in the same cluster we selected representative viruses genomes randomly from each country and from each host and constructed a final phylogenetic tree (Supplementary file 2). The topology of this tree showed that SARS-CoV-2 samples diverge from a common node close to the bat virus (Accession MN996532) and that all of them diverge from a common node very close to pangolin viruses (Accessions MT040333, MT040334, MT040335, MT040336, MT072864). From a distant node that contained the node of SARS-CoV-2 and also clustered a set of bat viruses, SARS virus diverges and grouped within a node together with Civets viruses, but also adjacent and very close to other bats viruses (Accession KY417146, KT444582 and KY417150). MERS viruses grouped in a different node also very close to other cluster containing bat viruses (Accession MF593268 and KC869678). Furthermore, adjacent to this node we found hedgehogs viruses (Accession KC545383, KC545386, MK679660, MK907286, MK907287 and NC\_039207).

For further analyses of molecular features and codon usage properties of viral genes, we selected the viruses according to the phylogenetic tree described above. First, we identified the 3 nodes containing the human viruses: SARS-CoV-2, SARS and MERS. Then we selected the closest viruses to each human virus within the nodes and classified them according to their hosts (bats, civets, hedgehogs and pangolins). From the human viruses only the references MERS (NC\_019843), SARS (NC\_004718) and SARS-CoV-2 (NC\_045512) were used. The total selected CDSs comprised 104 viral CDS.

### 3.2. Viral gene codon usage patterns

PCA of codon usage and molecular features of viral genes of SARS, MERS, SARS-CoV-2 and related viral genes of the non-human host (bats, civets, hedgehogs and pangolins) were performed in order to characterise the genes and distinguish important gene features among the viral gene families and species. PCA showed that the genes dispersed differentially according to the kind of gene rather than to the host that



the viruses infect. The genes distribution depending on the host was observed for only some genes (Figure 1 A and B). Most of the genes belonging to the same gene family overlapped or positioned in a very short ratio from each other. The position for nucleocapsid protein N is shared for all viruses except for SARS-CoV-2 that is the most distant from the group followed by the ones of SARS and MERS. Regarding the envelope protein E, the gene of civets SARS and human SARS occupied the same position while the gene of human SARS-CoV-2 and MERS distributed distantly from the group and also from each other. The genes that encode for the membrane glycoprotein M also showed a distribution along positive axis 1. However, for the human SARS-CoV-2 and hedgehog and bat MERS these genes distributed away from the genes of pangolin and bat SARS-CoV-2, human MERS and bat, civet and human SARS toward the inferior left quadrant. The main factors that contributed to the dispersion of these 3 genes (nucleocapsid protein N, envelope protein E and membrane glycoprotein M) were CBI, Fop, TrS2, C3, C3s, CpG and GC. In addition, the membrane glycoprotein M seems to be more influenced by the codon frequency of the codon TAC for Tyrosine and CTG for Lysine. Whereas for hedgehogs MERS and human SARS-CoV-2 the codons TAT for Tyrosine and TTA for Lysine as well as the GC bias, among others contributed most. All of them are strongly influenced by the A/T composition in the third codon position. On the other hand, the spike proteins S of all viruses distributed toward positive values of PC2 and were also highly influenced by the A/T composition in the third codon position. All these genes grouped very closely except for the gene of bats and human MERS. Several ORF proteins occupied the same area overlapping or positioning very close to each other. Other ORF genes such as ORF6, ORF8 and ORF3 of the human virus SARS-CoV-2 distributed distantly.

The CUB was estimated based on ENc values. The values of ENc range from 20 (when only one codon is used per amino acid) to 61 (when all codons are used with equal probability). Genes whose ENc values are lower than 50 are considered to have skewed codon usage. All viruses presented a wide range of ENc values ( $26 < ENc < 58$ ) that varied mainly depending on the type of genes. The highest ENc median was observed for the human MERS ( $ENc \sim 50.40$ ), followed by bats MERS ( $ENc \sim 49.64$ ). The hedgehogs MERS showed an ENc median of 47.70, being closer to the values that SARS and SARS-CoV-2 presented. Civets SARS showed an ENc median of 47.76. For bats SARS the ENc median was 47.80 and the ENc median for the human SARS was 47.66. The lowest ENc values were observed for the genes of SARS-CoV-2 viruses.

294 Bats SARS-CoV-2 showed a median ENc of 46.39. For pangolins SARS-CoV-2, the  
295 ENc median was 44.80 and for the human SARS-CoV-2, the ENc median was 44.34  
296 (Figure 1 C).

297 Codon bias of viral genes classified by the type of gene or the gene  
298 family showed that the envelope protein E presented ENc values that ranged from 42 to  
299 61, being the genes of the human SARS-CoV-2 and bat SARS-CoV-2 the ones that  
300 presented the lowest values of all the genes. Membrane glycoprotein M genes presented  
301 ENc values that ranged from 43.32 to 61.00, and the gene of hedgehogs MERS, the one  
302 with the lowest value. The membrane glycoprotein M of Human MERS, Civets, bats and  
303 human SARS showed virtually non-biased codon usage. The nucleocapsid protein N  
304 showed ENc values that ranged from 49.08 to 55.30 being the human MERS gene,  
305 followed by the bats MERS gene, the viral genes that presented the lowest values.

306 The genes that encode for the spike protein S presented ENc values that ranged  
307 from 44.16 to 47.68. The gene of the human SARS-CoV-2 showed the lowest ENc value  
308 followed by the genes of bat and pangolin SARS-CoV-2. ORF genes presented ENc  
309 values that ranged from 26.60 to 57.89, being the human SARS-CoV-2 the virus that  
310 presented the lowest and the highest ENc value for ORF7 and ORF10 respectively.

### 311 **3.3. CPB analysis between viruses and lung tissue highly expressed genes**

312 Since human viruses have codon usage biases that match highly expressed  
313 proteins in the tissues they infect (Miller et al., 2017) we selected the highly expressed  
314 genes in lungs tissue to compare the gene molecular features, CUB and CPB of SARS,  
315 SARS-CoV-2 and MERS viruses in relation with human genes. Since viruses replicate  
316 exclusively inside living cells, many viruses are influenced by host codon pair  
317 preferences, being the reflection of the CPB or CPS of their hosts. Therefore, CPS of viral  
318 genes was evaluated and compared with the CPS of human genes in order to determine  
319 whether viruses that infect humans have similar codon pair preferences to their  
320 host. Viral genes showed lower CPS frequencies than human genes. The median CPS for  
321 the viral genes was 0.053 for civet SARS, 0.051 for bat SARS, and 0.053 for human  
322 SARS. The median CPS that presented the MERS genes was 0.048 for hedgehog MERS,  
323 0.046 for bat MERS and 0.037 for human MERS. SARS-CoV-2 showed median CPS  
324 values of 0.064 for bat SARS-CoV-2, 0.065 for pangolins SARS-CoV-2 and 0.061 for  
325 human SARS-CoV-2. The median CPS for highly expressed human genes in lungs was  
326 0.11 (Figure 2A). We also calculated the median CPS of viral genes for each gene

family. The genes that encode for ORF7b and spike protein S were the genes with the highest median of CPB values (0.081 and 0.061 respectively), followed by ORF3a and nucleocapsid protein N (0.058 and 0.057) indicating that particular codon pairs are overrepresented in these genes. Envelope protein E and the membrane glycoprotein M showed values of 0.048 and 0.044 respectively (Figure 2B).

Furthermore, different CPB among the viral genes families of different virusesspecies that infect different hostswere also observed (Figure 2C). Bat SARS showed the highest CPB for ORF7b (~0.1) and ORF7a (~0.048). The human SARS-CoV-2 showed the highest CPB values for ORF1a (0.089), ORF1ab (0.051), nucleocapsid protein N (0.048) and spike protein S (0.042). Envelope protein E and membrane glycoprotein M presented CPB values of 0.0005 and 0.02 respectively. In pangolin SARS-CoV-2 the highest CPB value was for the spike protein S (0.060) followed by ORF3a (0.037) and ORF8 (0.033) while inbat SARS-CoV-2 the highest CPB value was for the spike protein S (0.076) followed by ORF1ab (0.050).The highest CPB values for human MERS genes were observedfor a non-structural protein (0.032) followed by the spike protein S (0.021) and the nucleocapsid protein N (0.008). In bat MERS the highest CPB value was for spike protein S(0.062) followed by ORF1a (0.022)and by the membrane glycoprotein M (0.022).In hedgehog MERS the highest CPB value was for ORF3a (0.049), followed by ORF1a/b (0.042)and the membrane glycoprotein M (0.029).In orderto evaluate the fitness and specialization of the viruses in theirhosts, we compared the CPS of the viral genes derived from the different hosts against the CPS of highly expressed genes in human lungs tissue by performing CPS correlation analysis. The 3721 codon pairs of all viruses were compared with the 3721 codon pairs of human genes. Correlation analyses showed low R values with a not clear dependence on the human host codon pairs (Supplementaryfile3).

### 3.4. Viral genes clustering analysis

Further analysis using hierarchical clustering of viral genes provided additional qualitative information about how similar certain genes are in terms of molecular and codon usage parameters(Supplementaryfile4). All the genes encoding for viral nucleocapsid protein N of all the virusesgrouped together demonstrating a high level of conservation. The human SARS-CoV-2 gene presented a very low CPB value in comparison with the genes of the other viruses.

Envelope protein E genes grouped in different clusters. The three SARS viruses (civets, bats and human hosts) grouped with the bat and pangolin SARS-CoV-2 and showed high and similar CPB values. Whereas the human SARS-CoV-2 grouped better with the human and bat MERS, both showing high CPB values. Hedgehog envelope protein E gene grouped distantly with ORF and hypothetical proteins. These genes presented a high preference for the codon GCG for Alanine. Furthermore, the codons GGT and CCT were preferable for Glycine and Proline respectively. The hydrophobicity, CAI and Fop values are higher for SARS and SARS-CoV-2 genes.

The membrane glycoprotein M genes also appeared in different clusters. The human SARS-CoV-2 gene grouped with the human and bat MERS gene. Only the human SARS-CoV-2 gene showed a preference for the codon GCA for Alanine and AGG for Arginine. A preference for the codons CCA, ACT and GTT for Proline, Threonine and Tyrosine was also observed. However, this was the gene that presented the lowest CPB value. The pangolin and bat SARS-CoV-2 gene grouped with the three SARS genes in a different cluster and showed a higher CPB. The hedgehogs MERS grouped distantly. The codon CAC was observed more frequently for Histidine in the three SARS viruses. Pangolin SARS-CoV-2 showed a preference for GAC for Aspartate and CCA for Proline whereas the bat SARS-CoV-2 showed a preference for GGA for Glycine and GTA for Valine.

The genes encoding for the spike protein S appeared in different clusters. For the human SARS-CoV-2, this gene grouped alone with the genes that encode for hypothetical and ORF proteins and showed high bias only for the codon TTG for Lysine and GAA for Glutamate. The genes for the rest of the viruses clustered together with other ORF genes and with the membrane glycoprotein M of hedgehogs, although distantly. This analysis also showed that CPB is highly related to the dinucleotide bias. In this cluster the genes that encode for the ORF genes showed low values of CPB, being the lowest of all the clusters. Conversely, the genes that encode for the spike protein S presented high CPB values.

### 3.5. Viral and human genes clustering analysis and CPS correlation analysis

Since virus fitness specialization could be dependent on the translation machinery for only some particular genes, we performed clustering analysis based on the codon usage and molecular features including human genes and the genes of

393 SARS-CoV-2, SARS and MERS(Supplementary file 1). From a total of 463 human  
394 genes, 70 genes (15.1%)grouped in clusters together with viral genes. These genes were  
395 selectedand extracted to make an illustrating heatmap including both, human and all  
396 viral genes (Figure 3).Furthermore, in order to figure out whether the viral genes that  
397 composed particular clusters present codon pair frequencies that correlate with the  
398 human genes of the same clusters, we evaluated the CPS of both, viral and human genes  
399 for each block and the correlation between each other.

400 For SARS-CoV-2, 8 out of 12 genesgrouped with 40 human genes distributed in  
401 4 clusters. The first cluster comprised3 viral genes: the nucleocapsid protein N, ORF1a  
402 and ORF1ab together with 19 human genes: COL6A5 (3), OVCH1 (2), DNAH12 (2),  
403 ROS1 (3), SCN7A, RP1, ABCA13 (4) and LRRK2 (3) and the CPS correlation was  
404  $R=0.11$  ( $p\text{-val}=7.1\times 10^{-8}$ ). The CPB values for the human and viral genes were -0.04  
405 and 0.15 respectively. The second cluster contained 2 viral genes: the spike protein S  
406 and ORF7b together with 9 human genes: AGTR2, TMEM212, CALCRL, FMO2 (2),  
407 FAM216B, CXCL10, MMP13 and SLC6A14. For this group, the CPS correlation  
408 between viral and human genes was  $R=0.21$  ( $p\text{-val}=0.0027$ ) and the CPB values for the  
409 human and viral genes were 0.05 and 0.12 respectively. The third cluster grouped only 1  
410 viral gene, the envelope protein E, with 10 human genes: IFNG, ST8SIA6 (2),  
411 SLC39A8 (2), CDC20B (3) and DCSTAMP (2), and the CPS correlation between viral  
412 and human genes were $R=0.29$  ( $p\text{-val}=0.0052$ ) and the CPB values for the human and  
413 the viral genes were 0.25 and 0.16 respectively. In the fourth cluster 2 human genes,  
414 TSPAN19 (2)grouped with the viral genes ORF6 and ORF7a and showed a CPS  
415 correlation of  $R=0.5$  ( $p\text{-val}=0,0016$ ). The CPB values for the human and viral genes  
416 were 0.13 and 0.14 respectively.

417 For SARS virus (Supplementary file 5), 12 out of 14 genes grouped with 39  
418 human genes distributed in 5 clusters. The first cluster contained 11 human genes:  
419 AGTR2, TMEM212, CALCRL, FMO2 (2), FAM216B, CXCL10, MMP13, SLC6A14,  
420 and BCL2A1 (2) and 7 viral genes: envelope protein E, hypothetical proteins (5) and  
421 membrane glycoprotein M.The CPS correlation for human and viral genes was  
422  $R=0.28$  ( $p\text{-val}=2\times 10^{-16}$ ). The second cluster was composed of 7 human genes:  
423 C7orf77, SNTN (2), MUC1 (2) and WIF1 (2).The CPS correlation between human and  
424 viral genes was  $R=0.77$  ( $p\text{-val}=0.00078$ ). The third cluster consisted of 19 human  
425 genes:  
426 COL6A5 (3), OVCH1 (2), DNAH12 (2), ROS1 (3), SCN7A, RP1, ABCA13 (4) and

LRRK2 (3) and 2 viral genes: ORF1a and ORF1ab. The CPS correlation between human and viral genes was  $R=0.31$  ( $p\text{-val}=2.2\times 10^{-16}$ ). The fourth cluster was composed of 2 TSPAN19 human genes and one viral hypothetical protein. CPS correlation for this cluster was statistically not significant.

For MERS virus (Supplementary file 6), the 10 genes grouped into 6 clusters together with 65 human genes. The first cluster comprised 19 human genes: COL6A5 (3), OVCH1 (2), DNAH12 (2), ROS1 (3), SCN7A, RP1, ABCA13 (4) and LRRK2 (3) and 2 viral genes: ORF1a and ORF1b. CPS correlation for human and viral genes was  $R=0.29$  ( $p\text{-val}=0.021$ ). The second cluster was composed of 8 human genes: AGTR2, TMEM212, CALCRL, FMO2 (2), CXCL10, MMP13 and SLC6A14 and 1 viral gene that encodes for the spike protein S. The third cluster contained 6 human genes: CLEC12A (3), FAM216B, DNAAF6 and PIH1D3 and 3 viral genes: non-structural protein (2) and the nucleocapsid protein N. The fourth cluster consisted of 7 human genes: C7orf77, SNTN(2), MUC1 (2) and WIF1 (2) and 1 viral gene encoding for a non-structural protein. The fifth cluster was composed of 9 human genes: ST8SIA6 (2), SLC39A8 (2), CDC20B (3) and DCSTAMP (2) and 2 viral genes: non-structural protein and membrane glycoprotein M. The sixth cluster comprised 16 human genes: CLEC6A, IL1RL1 (2), VNN2 (4), RTKN2 (2), SDR16C5 (3), IL18R1 (2), ACADL, and DNAH12 and the viral gene that encodes for envelope protein E.

Furthermore, we observed that 28 out of 70 human genes comprised a core of genes that appeared into the clusters together with the viral genes for the three human viruses (Figure 4 and Table 1). Between MERS and SARS-CoV-2 only 9 human genes were shared, 7 genes were shared between only MERS and SARS and 2 genes were shared between only SARS-CoV-2 and SARS. The 28 human genes that appeared in the clusters together with the genes of the 3 human viruses were retrieved against PheGenI (<https://www.ncbi.nlm.nih.gov/gap/phegeni/#pgGAP>) and DisGeNET (<https://www.disgenet.org/>) in order to classify the human diseases associated with the malfunction of the identified genes as an approach for possible human diseases or collateral effects caused by the viral infections (Supplementary file 1). According to PheGenI and DisGeNET, 14 out of the 28 genes were associated with 27 diseases. All the diseases appeared in nearly equal proportions. A slightly higher frequency was observed for Nervous System Diseases (12 genes), Neoplasms (12 genes), Respiratory Tract Diseases (11 genes), Pathological Conditions Signs and Symptoms (11 genes),



Neonatal Diseases and Abnormalities (11 genes) and Cardiovascular Diseases (10 genes) among others (Figure 4 B).

#### 4. Discussion

In humans, coronaviruses cause mainly respiratory tract infections. Previously, six coronaviruses were identified as human-susceptible viruses, being the  $\beta$ -coronaviruses, SARS-CoV and MERS-CoV, responsible for severe and potentially fatal respiratory tract infections (Yin and Wunderink, 2018). In December 2019 rising pneumonia cases caused by a novel  $\beta$ -coronavirus (SARS-CoV-2), occurred in Wuhan, China. The disease was officially named coronavirus disease 2019 (COVID-19). It was found that the genome sequence of SARS-CoV-2 is 96.2% identical to the bat coronavirus RaTG13, whereas it shares 79.5% of identity to SARS-CoV. It has been proposed that SARS-CoV-2 may have originated from bats or unknown intermediate hosts that could involve pangolins, crossing the species barrier into humans. (Guo et al., 2020). Rather, bats are the natural reservoir of a wide variety of coronaviruses, including SARS-CoV-like and MERS-CoV-like viruses (Banerjee et al., 2019; Hampton, 2005; Li et al., 2005).

Up to late April, a total of  $\approx$  500 SARS-CoV-2  $\beta$ -coronavirus genomes became available and this number is continuously increasing at an unprecedented rate. In our studies, we analysed the coronaviruses from different host species and retrieved the phylogeny in order to select the best candidate genomes for further analysis of codon usage and molecular relationship with the human host. As previously reported, we found that for SARS-CoV-2, SARS and MERS, bats seem to be a common natural host or reservoir.

Because viruses do not have tRNAs and rely on host cell machinery for replication, co-evolution between RNA viruses and their hosts' codon usages have been observed (Franzo et al., 2017; Rahman et al., 2018; Simón et al., 2017). Furthermore, the adaptation of viruses that replicates in multiple hosts should involve a trade-off between precise and functional matching to fit the diverse tRNA pools of multiple hosts (Tian et al., 2018). Conversely, single host viruses are expected to have specialised to match the host tRNA repertoire.

Since human viruses have CUB that matches highly expressed proteins in the tissues they infect (Miller et al., 2017) we selected the highly expressed genes in lung tissues to compare gene molecular features of SARS-CoV-2, SARS and MERS in



relation with human genes. In general, in our studies for all the analysed viruses we found that the total gene repertoire had a similar ENc average that differs only  $\pm 1$  unit with respect to their non-human host they come from, reflecting the molecular features of their original host. Furthermore, as demonstrated in our clustering analysis, codon pair usage seems to be dependent on the dinucleotide bias and the human CPB was higher for human genes than for viruses genes as previously reported (Kames et al., 2020; Kunec and Osterrieder, 2016).

Moreover, our analyses allowed us to distinguish not only the main factors that contribute to the distribution of the genes along the axes in PCA, but also to determine some particular different features among human and non-human viruses in specific genes that could be important for explaining the virus infection evolution. In contrast to SARS-CoV-2 of bats and pangolins, human SARS-CoV-2 exhibited a differential distribution in particular genes that depended mostly on the A/T content in the third codon position, which is in accordance with human SARS-CoV-2 gene composition reports (Alnazawi et al., 2017; Alonso and Diambra, 2020; Kames et al., 2020; Tort et al., 2020).

Important viral genes such as the membrane glycoprotein M, that is involved in the membrane transport of nutrients, the bud release, the formation of the envelope, the virus assembly and in the biosynthesis of new virus particles (Guo et al., 2020), distributed differentially from the non-human viruses indicating that it is highly influenced by A/T content. Surprisingly, this gene was positioned near of the hedgehog's MERS gene, suggesting similar molecular patterns between two distant viruses.

The envelope protein E, that functions as an ion channel and regulates virion assembly and the immune system of the host (Guo et al., 2020; Yin and Wunderink, 2018), showed the same tendency toward A/T ending codons for the human viruses SARS-CoV-2 and MERS. Human genes using A/T ending codons is also a common feature in several human genes since they present a wide rate of GC content (27-97%) (Bernardi, 2015; D'Onofrio et al., 1991). Both, membrane glycoprotein M and envelope protein E genes have a higher CUB in comparison with human MERS and SARS which is not in accordance with the trade-off theory that postulates that cross-species virus transmission demands relaxing the codon usage pattern (Kunec and Osterrieder, 2016). However, this phenomenon could be explained by a selection pressure in favour of the virus replication in the new host or due to the recent cross-species virus transmission as we know it occurred. If this is the case, the analysis of new isolates from infected humans

528 should tend to show incremented ENc values for the envelope protein E and membrane  
529 glycoprotein M genes.

530 Nevertheless, only the envelope protein E clustered together with human genes,  
531 demonstrating similar molecular patterns that could mean an advantage for virus  
532 replication in humans facilitating the virion assembly and the regulation of the immune  
533 system of the host. Furthermore, positive CPB and an incremented CPS correlation for  
534 the cluster that grouped the envelope protein E with human genes supports the  
535 hypothesis of a facilitated translation depending on codon usage and codon pairs.  
536 Similar patterns were observed for ORF6 and ORF8 genes, which are involved in the  
537 viral pathogenesis, apoptosis induction and inflammatory responses in the host (Chen et  
538 al., 2020b; Diemer et al., 2010). These genes grouped with human genes in different  
539 clusters and showed also an incremented CPS correlation.

540 Studies in different viruses species have reported high conservation of the genes  
541 that encode for the nucleocapsid protein N among virus families (HORNE, 2013; Kunec  
542 and Osterrieder, 2016; Masters, 2019; Nathan and Scobell, 2012; Parker and Masters,  
543 1990). Therefore, it is expected that codon usage and molecular patterns present similar  
544 features as observed in our studies. Nevertheless, SARS-CoV-2 nucleocapsid gene  
545 tends to distribute slightly far from the rest of viruses' capsids genes and toward a  
546 higher A/T content in PCA. Both, the human SARS and SARS-CoV-2 nucleocapsid  
547 protein N present high CPB suggesting a specialization acquirement in the human host.

548 Two viral genes that also present high CPB are ORF1a/b, that encodes for the  
549 replicase complex (polyproteins pp1a and pp1ab) and the Spike protein S that  
550 participates in the early viral infection by attaching to the host receptor ACE2 and  
551 mediating the internalization of the virus (Guo et al., 2020). In our studies, ORF1a/b  
552 grouped with the gene that encodes for the nucleocapsid protein N, indicating that their  
553 molecular features are highly conserved and are also present in several human genes.  
554 This result is in concordance with previous works that proposed these genes as  
555 candidates for deoptimization for the design of attenuated vaccines due to their high  
556 positive CPB values (Kames et al., 2020). Instead, the gene that encodes for the spike  
557 protein S, grouped with ORF7 (involved in viral pathogenesis and apoptosis induction)  
558 that also presents high and similar positive CPB values. For all of them, a higher rate of  
559 A/T composition in the third codon position was observed. Changes in the third position  
560 produce synonymous substitutions that could have conducted to a codon optimization in  
561 human cells using the host machinery that translates only genes whose molecular

562 features match the viral needs. Some viral genes seem to have been favoured for an  
 563 increased viral replication in humans and optimized by using or mimicking some  
 564 particular molecular patterns of human genes. But only some genes, such as the  
 565 envelope E, the ORF 6 and 8, could be the key for an exacerbated viral pathogenesis.  
 566 Furthermore, because of these molecular and codon usage similarities between some  
 567 highly expressed human genes and viral genes that occupy the same clusters, the  
 568 translation machinery of the host could propitiate the translation of viral genes to the  
 569 detriment of human gene expression in lung tissues. Indeed, mistranslation or de-  
 570 regulation of protein synthesis has been reported as a consequence of tRNA miss-  
 571 modification and imbalanced tRNA expression, causing diseases (Lant et al., 2019).  
 572 Recent studies have also proposed that an unbalance in the tRNAs pools of the infected  
 573 cells could occur and would explain the collateral effects observed in some viral  
 574 infections (Alonso and Diambra, 2020). Since COVID-19 outbreak, several studies  
 575 associated with different pathologies have been performed in order to find out how  
 576 damaging this new virus is for the human being. Hereby, in our studies we provided a  
 577 list of human genes that could be particularly affected as a consequence of their  
 578 molecular similarities with viral genes, not only belonging to SARS-CoV-2 but also to  
 579 SARS and MERS. The malfunction of these genes has been associated with different  
 580 human pathologies and is in continuous increase. Patients infected with COVID-19  
 581 typically present fever and respiratory symptoms. Nevertheless, it has been reported an  
 582 increased risk for complications of hypertension, congestive heart failure, and  
 583 atherosclerosis conducting to an increased presence of cardiovascular comorbidities  
 584 (Clerkin et al., 2020; Li et al., 2020; Zheng et al., 2020). Also, some patients have  
 585 experimented gastrointestinal manifestations (Wong et al., 2020), neurologic  
 586 complications (Bridwell et al., 2020; Dugue et al., 2020), and complications associated  
 587 with the endocrine and urogenital systems, among others (Wang et al., 2020; Wu et al.,  
 588 2020). Diseases and collateral effects caused by COVID-19 infections could be a  
 589 consequence of the malfunction of the genes listed in our work. Therefore, they should  
 590 be considered to be incorporated into susceptibility population studies for respiratory  
 591 viral infections. Hereby, these results lay the groundwork for further research in the field  
 592 of human genetics associated with the new viral infection, COVID-19, caused by  
 593 SARS-CoV-2 and for the development of antiviral preventive methods.

## 594 **5. Conclusions**

In our study, we described the main factors that shape CUB in SARS-CoV-2, SARS and MERS in comparison with highly expressed genes in human lung tissue and revealed matching features with human genes that could have favoured the virus for an incremented pathogenesis. Furthermore, we provided a list of candidate human genes that could be involved in the viral infection and had not been described yet which could be the key for explaining collateral effects and the human susceptibility to viral infections and should be considered to be incorporated into genetic population studies.

## 6. Declarations

### 6.1. Competing interests

The authors declare that the research was conducted in the absence of any commercial or financial relationships that could be construed as a potential conflict of interest.

### 6.2. Funding

This study was supported by the MinCyT CAPES BR/RED 1413 (L.K.), and Sistema Nacional de Computación de Alto Desempeño (SNCAD-MiNCyT) (L. K.).

### 6.3. Authors' contributions

L. K wrote and revised the manuscript L.M. designed the study, performed the bioinformatics analysis, wrote and revised the manuscript.

## Legends to figures

**Figure 1:** viral genes distribution in PCA plot in the first 2 axes and ENc-GC3s plot of SARS-CoV-2 (NC\_045512), SARS (NC\_004718) and MERS (NC\_038294), and the related virus of non-human hosts: Civets SARS (AY686864), bats MERS (KC869678), bats SARS (KY417150), bats SARS-CoV-2 (MN996532), pangolins SARS-CoV-2 (MT040336) and hedgehogs MERS (NC\_039207). **A).** Distribution of viral genes in PC1 and PC2. **B).** Main factors represented by vectors that contribute to the distribution of viral genes in PC1 and PC2. **C).** Distribution of the effective number of codons (ENc) in relation to the GC3s of viral genes. The standard curve of ENc is indicated in solid line.

**Figure 2:** codon pair score of viral genes of SARS-CoV-2 (NC\_045512), SARS

(NC\_004718) and MERS (NC\_038294), and the related virus of non-human hosts: civets SARS (AY686864), bats MERS (KC869678), bats SARS (KY417150), bats SARS-CoV-2 (MN996532), pangolins SARS-CoV-2 (MT040336) and hedgehogs MERS (NC\_039207) and human genes. **A).** codon pair frequencies for each virus. **B).** codon pair frequencies for each gene and classified by type of viral gene. **C).** Codon pair bias for each viral gene vs protein length.

**Figure 3:** Heatmap of clusters(1 to 4) using a hierarchical method of viral genes for SARS-CoV-2 (NC\_045512) of the human host and human genes based on the molecular features. CPB correlation is included in the left for each cluster relating the CPB of human genes (horizontal axis) and CPB of the viral genes (vertical axis).

**Figure 4: A).**Venn diagram representing the number of human genes that clustered together with viral genes for SARS-CoV-2 (NC\_045512), SARS (NC\_004718) and MERS (NC\_038294) based on the molecular features.**B).**Diseases frequencies associated to human genes grouped with viral genes of SARS-CoV-2, SARS and MERS in the clustering analysis.

## Tables

Table 1: Human genes shared among the clusters of the three coronaviruses SARS-CoV-2, SARS and MERS

Accession Id	Gene name	Proteins
NP_000677	AGTR2	type-2 angiotensin II receptor
NP_001157908	TMEM212	transmembrane protein 212
NP_001258680	CALCRL	calcitonin gene-related peptide type 1 receptor precursor
NP_001265227	COL6A5	collagen alpha-5(VI) chain isoform 1 precursor
NP_001288276	FMO2	dimethylaniline monooxygenase
NP_001305861	FAM216B	protein FAM216B
NP_001340108	OVCH1	ovochymase-1 precursor
NP_001352957	DNAH12	dynein heavy chain 12, axonemal isoform 4
NP_001365831	ROS1	proto-oncogenetyrosine-proteinkinase ROS isoform 3 precursor
NP_001451	FMO2	dimethylaniline monooxygenase
NP_001556	CXCL10	C-X-C motif chemokine 10 precursor
NP_002418	MMP13	collagenase 3 preproprotein
NP_002935	ROS1	proto-oncogenetyrosine-proteinkinase ROS isoform 1 precursor
NP_002967	SCN7A	sodium channel protein type 7 subunit alpha
NP_006260	RP1	oxygen-regulated protein 1 isoform 1
NP_009162	SLC6A14	sodium- and chloride-dependent neutral and basic amino acid transporter B(0+)
NP_689914	ABCA13	ATP-binding cassette sub-family A member 13
NP_694996	COL6A5	collagen alpha-5(VI) chain isoform 2 precursor
NP_940980	LRRK2	leucine-rich repeat serine/threonine-protein kinase 2

XP_005268686	LRRK2	leucine-rich repeat serine/threonine-protein kinase 2 isoform X1
XP_011510923	COL6A5	collagen alpha-5(VI) chain isoform X1
XP_011513433	ABCA13	ATP-binding cassette sub-family A member 13 isoform X2
XP_011513434	ABCA13	ATP-binding cassette sub-family A member 13 isoform X3
XP_011513438	ABCA13	ATP-binding cassette sub-family A member 13 isoform X6
XP_011534357	ROS1	proto-oncogene tyrosine-protein kinase ROS isoform X10
XP_011536184	LRRK2	leucine-rich repeat serine/threonine-protein kinase 2 isoform X8
XP_024100505	DNAH12	dynein heavy chain 12, axonemal isoform X2
XP_024304736	OVCH1	ovochoymase-1 isoform X1

641

## 642 **Legends to supplementary files**

643 **Supplementary file 2:** Phylogenetic tree using 118 virus genomes including the  
644 references SARS-CoV-2, SARS, and MERS and related viruses belonging to non-  
645 human host as described in Supplementary file 1. The clusters were virus grouped with  
646 SARS-CoV-2, SARS, and MERS are highlighted. The accession id is followed by the  
647 host the sample was isolated from or the county in the case of different isolation of  
648 SARS-CoV-2.

649 **Supplementary file 3:** Codon pair bias plots and correlation of viral genes  
650 against highly expressed human genes in lungs tissues according to the fold-change  
651 between the expression level in lung and the tissue with second-highest expression level  
652 according to “Human Protein Atlas”  
653 (<https://www.proteinatlas.org/humanproteome/tissue/lung>). P1: KT444582, P2:  
654 KY417146, P3: KY417150, P4: MG772934, P5: MN996532, P6: C869678, P7:  
655 MF593268, P8: FJ938064, P9: FJ938066, P10: KX432213, P11: Y572035, P12:  
656 AY686864, P13: MK679660, P14: NC\_039207, P15: NC\_038294, P16: T040336, P17:  
657 MT040333, P18: MT126808, P19: NC\_045512, P20: MT066156, P21: T263074, P22:  
658 NC\_004718, P23: MT198652, P24: MT233519, P25: MT233523, P26: T118835, P27:  
659 MT233526, P28: MT259235, P29: MT263435.

660 **Supplementary file 4:** Heatmaps clustering using a hierarchical method of viral  
661 genes based on the measures of molecular and codon usage patterns. The viruses whose  
662 genes were included here were SARS-Cov-2, SARS, and MERS and the closest viruses  
663 to the common nodes in the phylogenetic tree of supplementary file 2. Civets SARS  
664 (AY686864), bats MERS (KC869678), bats SARS (KY417150), bats SARS-CoV-2  
665 (MN996532), pangolins SARS-CoV-2 (MT040336), human SARS (NC\_004718),  
666 human MERS (NC\_038294), hedgehogs MERS (NC\_039207) and the human SARS-

667 CoV-2 (NC\_045512).

668 **Supplementary file 5:** Heatmap of clusters (1 to 4) using a hierarchical method  
669 of viral genes for SARS (NC\_004718) of the human host and human genes based on the  
670 molecular features. CPB correlation is included in the left for each cluster relating the  
671 CPB of human genes (horizontal axis) and CPB of the viral genes (vertical axis).

672 **Supplementary file 6:** Heatmap of clusters (1 to 6) using a hierarchical method  
673 of viral genes for SARS (NC\_038294) of the human host and human genes based on the  
674 molecular features. CPB correlation is included in the left for each cluster relating the  
675 CPB of human genes (horizontal axis) and CPB of the viral genes (vertical axis).

## 676 7. References

677 Alnazawi, M., Altaher, A., and Kandeel, M. (2017). Comparative genomic analysis  
678 MERS CoV isolated from humans and camels with special reference to virus  
679 encoded helicase. *Biol. Pharm. Bull.* 40, 1289–1298. doi:10.1248/bpb.b17-00241.

680 Alonso, A. M., and Diambra, L. (2020). SARS-CoV-2 codon usage bias downregulates  
681 host expressed genes with similar codon usage. *bioRxiv*, 2020.05.05.079087.  
682 doi:10.1101/2020.05.05.079087.

683 Banerjee, A., Kulcsar, K., Misra, V., Frieman, M., and Mossman, K. (2019). Bats and  
684 coronaviruses. *Viruses* 11. doi:10.3390/v11010041.

685 Bennetzen, J. L., and Hall, B. D. (1982). Codon selection in yeast. *J. Biol. Chem.* 257,  
686 3026–3031. Available at: <http://www.jbc.org/content/257/6/3026.full.pdf>  
687 [Accessed September 11, 2017].

688 Bernardi, G. (2015). Chromosome Architecture and Genome Organization. *PLoS One*  
689 10, e0143739. doi:10.1371/journal.pone.0143739.

690 Bridwell, R., Long, B., and Gottlieb, M. (2020). Neurologic complications of COVID-  
691 19. *Am. J. Emerg. Med.* doi:10.1016/j.ajem.2020.05.024.

692 Cavanagh, D. (2007). Coronavirus avian infectious bronchitis virus. *Vet. Res.* 38, 281–  
693 297. doi:10.1051/vetres:2006055.

694 Chan, J. F. W., Kok, K. H., Zhu, Z., Chu, H., To, K. K. W., Yuan, S., et al. (2020).  
695 Genomic characterization of the 2019 novel human-pathogenic coronavirus



696 isolated from a patient with atypical pneumonia after visiting Wuhan. *Emerg.*  
697 *Microbes Infect.* 9, 221–236. doi:10.1080/22221751.2020.1719902.

698 Chen, Y., Liu, Q., and Guo, D. (2020a). Emerging coronaviruses: Genome structure,  
699 replication, and pathogenesis. *J. Med. Virol.* 92, 418–423. doi:10.1002/jmv.25681.

700 Chen, Y., Liu, Q., and Guo, D. (2020b). Emerging coronaviruses: Genome structure,  
701 replication, and pathogenesis. *J. Med. Virol.* 92, 418–423. doi:10.1002/jmv.25681.

702 Clark, M. A. (1993). Bovine coronavirus. *Br. Vet. J.* 149, 51–70. doi:10.1016/S0007-  
703 1935(05)80210-6.

704 Clerkin, K. J., Fried, J. A., Raikhelkar, J., Sayer, G., Griffin, J. M., Masoumi, A., et al.  
705 (2020). Coronavirus Disease 2019 (COVID-19) and Cardiovascular Disease.  
706 *Circulation*. doi:10.1161/CIRCULATIONAHA.120.046941.

707 Coleman, J. R., Papamichail, D., Skiena, S., Fitcher, B., Wimmer, E., and Mueller, S.  
708 (2008). Virus Attenuation by Genome-Scale Changes in Codon Pair Bias. *Science*  
709 (80-. ). 320, 1784–1787. doi:10.1126/science.1155761.

710 Cui, J., Li, F., and Shi, Z. L. (2019). Origin and evolution of pathogenic coronaviruses.  
711 *Nat. Rev. Microbiol.* 17, 181–192. doi:10.1038/s41579-018-0118-9.

712 D’Onofrio, G., Mouchiroud, D., Aïssani, B., Gautier, C., and Bernardi, G. (1991).  
713 Correlations between the compositional properties of human genes, codon usage,  
714 and amino acid composition of proteins. *J. Mol. Evol.* 32, 504–510.  
715 doi:10.1007/BF02102652.

716 Diemer, C., Schneider, M., Schätzl, H. M., and Gilch, S. (2010). “Modulation of host  
717 cell death by SARS coronavirus proteins,” in *Molecular Biology of the SARS-*  
718 *Coronavirus* (Springer Berlin Heidelberg), 231–245. doi:10.1007/978-3-642-  
719 03683-5\_14.

720 Dugue, R., Cay-Martínez, K. C., Thakur, K., Garcia, J. A., Chauhan, L. V., Williams, S.  
721 H., et al. (2020). Neurologic manifestations in an infant with COVID-19.  
722 *Neurology*, 10.1212/WNL.0000000000009653.  
723 doi:10.1212/wnl.0000000000009653.

- 724 Franzo, G., Tucciarone, C. M., Cecchinato, M., and Drigo, M. (2017). Canine  
725 parvovirus type 2 (CPV-2) and Feline panleukopenia virus (FPV) codon bias  
726 analysis reveals a progressive adaptation to the new niche after the host jump. *Mol.*  
727 *Phylogenet. Evol.* 114, 82–92. doi:10.1016/j.ympev.2017.05.019.
- 728 Gouy, M., and Gautier, C. (1982). Codon usage in bacteria: Correlation with gene  
729 expressivity. *Nucleic Acids Res.* 10, 7055–7074. doi:10.1093/nar/10.22.7055.
- 730 Greenacre, M. J. (1984). *Theory and applications of correspondence analysis.*  
731 Academic Press Available at:  
732 [https://books.google.com.ar/books/about/Theory\\_and\\_Applications\\_of\\_Correspon](https://books.google.com.ar/books/about/Theory_and_Applications_of_Correspondence.html?id=LsPaAAAAMAAJ&redir_esc=y)  
733 [denc.html?id=LsPaAAAAMAAJ&redir\\_esc=y](https://books.google.com.ar/books/about/Theory_and_Applications_of_Correspondence.html?id=LsPaAAAAMAAJ&redir_esc=y) [Accessed May 27, 2018].
- 734 Guo, Y. R., Cao, Q. D., Hong, Z. S., Tan, Y. Y., Chen, S. D., Jin, H. J., et al. (2020).  
735 The origin, transmission and clinical therapies on coronavirus disease 2019  
736 (COVID-19) outbreak- A n update on the status. *Mil. Med. Res.* 7, 1–10.  
737 doi:10.1186/s40779-020-00240-0.
- 738 Hampton, T. (2005). Bats may be SARS reservoir. *J. Am. Med. Assoc.* 294, 2291.  
739 doi:10.1001/jama.294.18.2291.
- 740 Hartl, D. L., Moriyama, E. N., and Sawyer, S. A. (1994). Selection intensity for codon  
741 bias. *Genetics* 138, 227–234. doi:10.3168/jds.S0022-0302(75)84789-8.
- 742 HORNE, R. W. (2013). “The Structure of Viruses,” in *Scientific American* (Elsevier),  
743 153–178. doi:10.1090/gsm/146/03.
- 744 Ikemura, T. (1981). Correlation between the abundance of Escherichia coli transfer  
745 RNAs and the occurrence of the respective codons in its protein genes: A proposal  
746 for a synonymous codon choice that is optimal for the E. coli translational system.  
747 *J. Mol. Biol.* 151, 389–409. doi:10.1016/0022-2836(81)90003-6.
- 748 Kames, J., Holcomb, D. D., Kimchi, O., DiCuccio, M., Hamasaki-Katagiri, N., Wang,  
749 T., et al. (2020). Sequence analysis of SARS-CoV-2 genome reveals features  
750 important for vaccine design. *bioRxiv*, 2020.03.30.016832.  
751 doi:10.1101/2020.03.30.016832.

- 752 Kunec, D., and Osterrieder, N. (2016). Codon Pair Bias Is a Direct Consequence of  
753 Dinucleotide Bias. *Cell Rep.* 14, 55–67. doi:10.1016/j.celrep.2015.12.011.
- 754 Lanfear, R., Frandsen, P. B., Wright, A. M., Senfeld, T., and Calcott, B. (2016).  
755 PartitionFinder 2: New Methods for Selecting Partitioned Models of Evolution for  
756 Molecular and Morphological Phylogenetic Analyses. *Mol. Biol. Evol.* 34,  
757 msw260. doi:10.1093/molbev/msw260.
- 758 Lant, J. T., Berg, M. D., Heinemann, I. U., Brandl, C. J., and O'Donoghue, P. (2019).  
759 Pathways to disease from natural variations in human cytoplasmic tRNAs. *J. Biol.*  
760 *Chem.* 294, 5294–5308. doi:10.1074/jbc.REV118.002982.
- 761 Lee, S., Weon, S., Lee, S., and Kang, C. (2010). Relative codon adaptation index, a  
762 sensitive measure of codon usage bias. *Evol. Bioinforma.* 2010, 47–55.  
763 doi:10.4137/EBO.S4608.
- 764 Li, B., Yang, J., Zhao, F., Zhi, L., Wang, X., Liu, L., et al. (2020). Prevalence and  
765 impact of cardiovascular metabolic diseases on COVID-19 in China. *Clin. Res.*  
766 *Cardiol.* 109, 531–538. doi:10.1007/s00392-020-01626-9.
- 767 Li, W., Shi, Z., Yu, M., Ren, W., Smith, C., Epstein, J. H., et al. (2005). Bats are natural  
768 reservoirs of SARS-like coronaviruses. *Science* (80-. ). 310, 676–679.  
769 doi:10.1126/science.1118391.
- 770 Lobry, J. R., and Gautier, C. (1994). Hydrophobicity, expressivity and aromaticity are  
771 the major trends of amino-acid usage in 999 escherichia coli chromosome-encoded  
772 genes. *Nucleic Acids Res.* 22, 3174–3180. doi:10.1093/nar/22.15.3174.
- 773 Masters, P. S. (2019). Coronavirus genomic RNA packaging. *Virology* 537, 198–207.  
774 doi:10.1016/j.virol.2019.08.031.
- 775 Miller, J. B., Hippen, A. A., Wright, S. M., Morris, C., and Ridge, P. G. (2017). Human  
776 viruses have codon usage biases that match highly expressed proteins in the tissues  
777 they infect. *Res. Artic. Biomed. Genet. Genomics* 2, 1–5.  
778 doi:10.15761/BGG.1000134.
- 779 Mueller, S., Coleman, J. R., Papamichail, D., Ward, C. B., Nimnual, A., Futcher, B., et

al. (2010). Live attenuated influenza virus vaccines by computer-aided rational design. *Nat. Biotechnol.* 28, 723–726. doi:10.1038/nbt.1636.

Nathan, A. J., and Scobell, A. (2012). How China sees America. *Foreign Aff.* 91, 287. doi:10.1017/CBO9781107415324.004.

Nouën, C. Le, Brock, L. G., Luongo, C., McCarty, T., Yang, L., Mehedi, M., et al. (2014). Attenuation of human respiratory syncytial virus by genome-scale codon-pair deoptimization. *Proc. Natl. Acad. Sci. U. S. A.* 111, 13169–13174. doi:10.1073/pnas.1411290111.

Novembre, J. A. (2002). Accounting for Background Nucleotide Composition When Measuring Codon Usage Bias. *Mol. Biol. Evol.* 19, 1390–1394. doi:10.1093/oxfordjournals.molbev.a004201.

Parker, M. M., and Masters, P. S. (1990). Sequence comparison of the N genes of five strains of the coronavirus mouse hepatitis virus suggests a three domain structure for the nucleocapsid protein. *Virology* 179, 463–468. doi:10.1016/0042-6822(90)90316-J.

Peden, J. F. (1999). Analysis of codon usage. *Biosystems.* 5. doi:10.1016/j.biosystems.2011.06.005.

Peiris, J. S. M., Guan, Y., and Yuen, K. Y. (2004). Severe acute respiratory syndrome. *Nat. Med.* 10, S88–S97. doi:10.1038/nm1143.

Price, M. N., Dehal, P. S., and Arkin, A. P. (2009). Fasttree: Computing large minimum evolution trees with profiles instead of a distance matrix. *Mol. Biol. Evol.* 26, 1641–1650. doi:10.1093/molbev/msp077.

Rahman, S. U., Yao, X., Li, X., Chen, D., and Tao, S. (2018). Analysis of codon usage bias of Crimean-Congo hemorrhagic fever virus and its adaptation to hosts. *Infect. Genet. Evol.* 58, 1–16. doi:10.1016/j.meegid.2017.11.027.

Sharp, P. M., and Li, W. H. (1987). The codon adaptation index-a measure of directional synonymous codon usage bias, and its potential applications. *Nucleic Acids Res.* 15, 1281–1295. doi:10.1093/nar/15.3.1281.

808 Shen, S. H., Stauff, C. B., Gorbatshevych, O., Song, Y., Ward, C. B., Yurovsky, A., et al.  
809 (2015). Large-scale recoding of an arbovirus genome to rebalance its insect versus  
810 mammalian preference. *Proc. Natl. Acad. Sci. U. S. A.* 112, 4749–4754.  
811 doi:10.1073/pnas.1502864112.

812 Sievers, F., Wilm, A., Dineen, D., Gibson, T. J., Karplus, K., Li, W., et al. (2011). Fast,  
813 scalable generation of high-quality protein multiple sequence alignments using  
814 Clustal Omega. *Mol. Syst. Biol.* 7, 539. doi:10.1038/msb.2011.75.

815 Simón, D., Fajardo, A., Sónora, M., Delfraro, A., and Musto, H. (2017). Host influence  
816 in the genomic composition of flaviviruses: A multivariate approach. *Biochem.*  
817 *Biophys. Res. Commun.* 492, 572–578. doi:10.1016/j.bbrc.2017.06.088.

818 Su, S., Wong, G., Shi, W., Liu, J., Lai, A. C. K., Zhou, J., et al. (2016). Epidemiology,  
819 Genetic Recombination, and Pathogenesis of Coronaviruses. *Trends Microbiol.* 24,  
820 490–502. doi:10.1016/j.tim.2016.03.003.

821 Sueoka, N. (1988). Directional mutation pressure and neutral molecular evolution. *Proc.*  
822 *Natl. Acad. Sci. U. S. A.* 85, 2653–2657. doi:10.1073/pnas.85.8.2653.

823 Suzuki, H., Saito, R., and Tomita, M. (2005). A problem in multivariate analysis of  
824 codon usage data and a possible solution. *FEBS Lett.* 579, 6499–6504.  
825 doi:10.1016/j.febslet.2005.10.032.

826 Tian, L., Shen, X., Murphy, R. W., and Shen, Y. (2018). The adaptation of codon usage  
827 of +ssRNA viruses to their hosts. *Infect. Genet. Evol.* 63, 175–179.  
828 doi:10.1016/j.meegid.2018.05.034.

829 Tort, F. L., Castells, M., and Cristina, J. (2020). A comprehensive analysis of genome  
830 composition and codon usage patterns of emerging coronaviruses. *Virus Res.* 283.  
831 doi:10.1016/j.virusres.2020.197976.

832 Uddin, A., and Chakraborty, S. (2018). Codon Usage Pattern of Genes Involved in  
833 Central Nervous System. *Mol. Neurobiol.* doi:10.1007/s12035-018-1173-y.

834 Uddin, A., Choudhury, M. N., and Chakraborty, S. (2017). Factors influencing codon  
835 usage of mitochondrial ND1 gene in pisces, aves and mammals. *Mitochondrion* 37,

836 17–26. doi:10.1016/j.mito.2017.06.004.

837 Wang, B., Yang, C., Tekes, G., Mueller, S., Paul, A., Whelan, S. P. J., et al. (2015).  
838 Recoding of the vesicular stomatitis virus L gene by computer-aided design  
839 provides a live, attenuated vaccine candidate. *MBio* 6. doi:10.1128/mBio.00237-  
840 15.

841 Wang, L. F., Shi, Z., Zhang, S., Field, H., Daszak, P., and Eaton, B. T. (2006). Review  
842 of bats and SARS. *Emerg. Infect. Dis.* 12, 1834–1840.  
843 doi:10.3201/eid1212.060401.

844 Wang, S., Zhou, X., Zhang, T., and Wang, Z. (2020). The need for urogenital tract  
845 monitoring in COVID-19. *Nat. Rev. Urol.* doi:10.1038/s41585-020-0319-7.

846 Wong, A., Li, X., Lau, S., and Woo, P. (2019). Global Epidemiology of Bat  
847 Coronaviruses. *Viruses* 11, 174. doi:10.3390/v11020174.

848 Wong, S. H., Lui, R. N., and Sung, J. J. (2020). Covid-19 and the digestive system. *J.*  
849 *Gastroenterol. Hepatol.* 35, 744–748. doi:10.1111/jgh.15047.

850 Wright, F. (1990). The “effective number of codons” used in a gene. *Gene* 87, 23–29.  
851 doi:10.1016/0378-1119(90)90491-9.

852 Wu, Z., Zhang, Z., and Wu, S. (2020). Focus on the Crosstalk Between COVID-19 and  
853 Urogenital Systems. *J. Urol.* doi:10.1097/ju.0000000000001068.

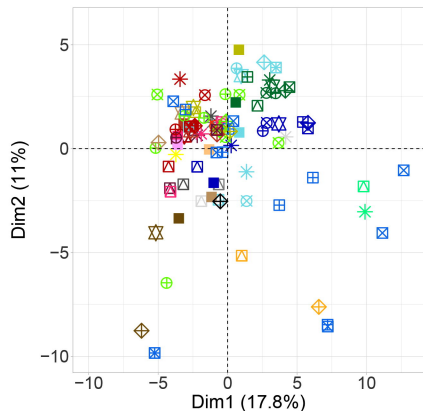
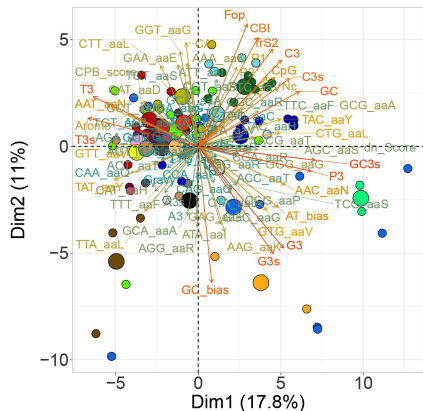
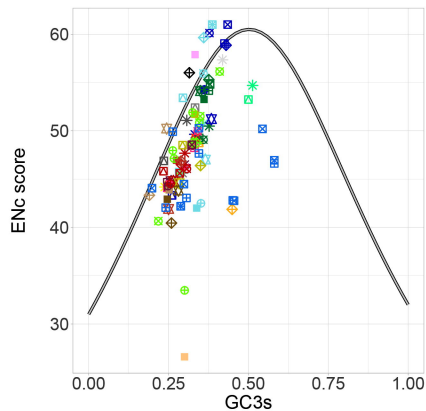
854 Yang, C., Skiena, S., Fitcher, B., Mueller, S., and Wimmer, E. (2013). Deliberate  
855 reduction of hemagglutinin and neuraminidase expression of influenza virus leads  
856 to an ultraproductive live vaccine in mice. *Proc. Natl. Acad. Sci. U. S. A.* 110,  
857 9481–9486. doi:10.1073/pnas.1307473110.

858 Yin, Y., and Wunderink, R. G. (2018). MERS, SARS and other coronaviruses as causes  
859 of pneumonia. *Respirology* 23, 130–137. doi:10.1111/resp.13196.

860 Zaki, A. M., van Boheemen, S., Bestebroer, T. M., Osterhaus, A. D. M. E., and  
861 Fouchier, R. A. M. (2012). Isolation of a Novel Coronavirus from a Man with  
862 Pneumonia in Saudi Arabia. *N. Engl. J. Med.* 367, 1814–1820.  
863 doi:10.1056/NEJMoa1211721.

- 864 Zheng, Y. Y., Ma, Y. T., Zhang, J. Y., and Xie, X. (2020). COVID-19 and the  
 865 cardiovascular system. *Nat. Rev. Cardiol.* 17, 259–260. doi:10.1038/s41569-020-  
 866 0360-5.
- 867 Zhou, P., Fan, H., Lan, T., Yang, X. Lou, Shi, W. F., Zhang, W., et al. (2018). Fatal  
 868 swine acute diarrhoea syndrome caused by an HKU2-related coronavirus of bat  
 869 origin. *Nature* 556, 255–259. doi:10.1038/s41586-018-0010-9.



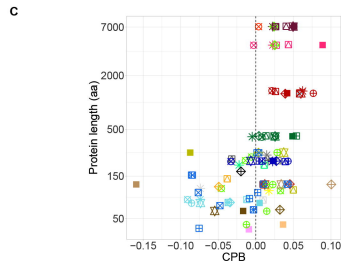
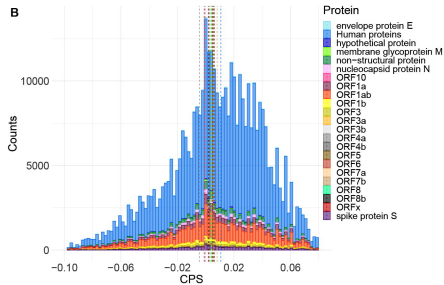
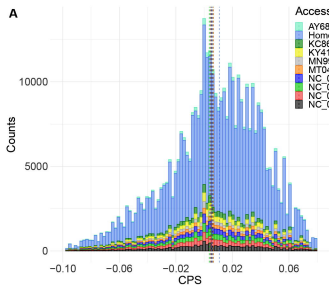
**A****B****C**

### Proteins

- |                           |                   |
|---------------------------|-------------------|
| ● envelope protein E      | ● ORF3b           |
| ● hypothetical protein    | ● ORF4a           |
| ● membrane glycoprotein M | ● ORF4b           |
| ● non-structural protein  | ● ORF5            |
| ● nucleocapsid protein N  | ● ORF6            |
| ● ORF10                   | ● ORF7a           |
| ● ORF1a                   | ● ORF7b           |
| ● ORF1ab                  | ● ORF8            |
| ● ORF1b                   | ● ORF8b           |
| ● ORF3                    | ● ORFx            |
| ● ORF3a                   | ● spike protein S |

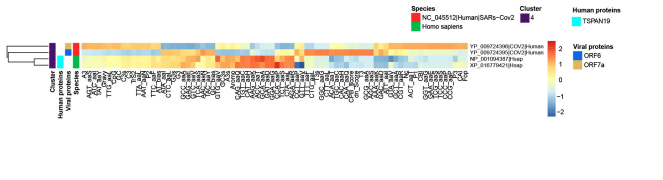
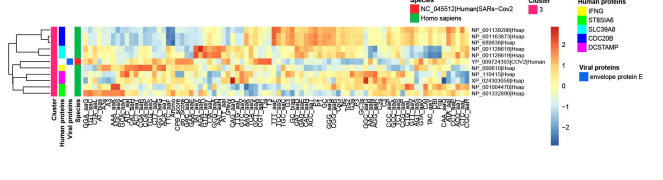
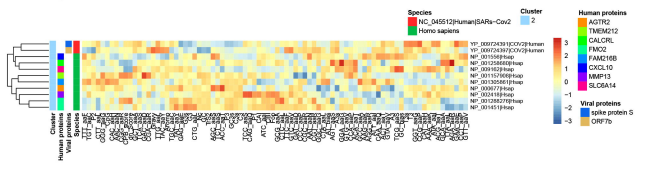
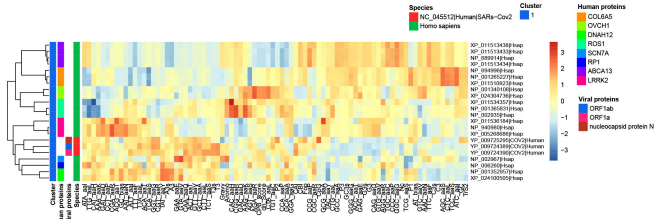
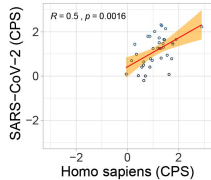
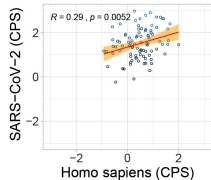
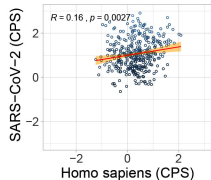
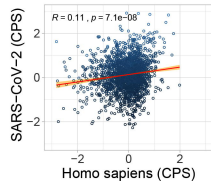
### Accession | Host | Virus

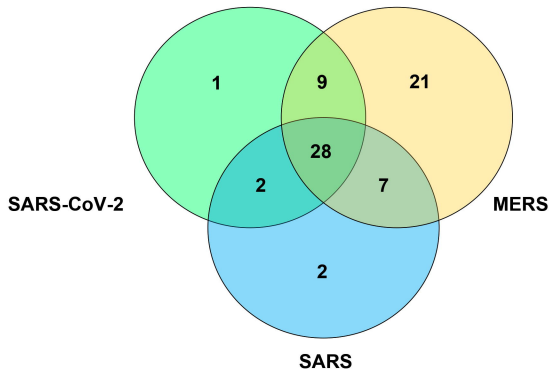
- |   |                               |
|---|-------------------------------|
| ⊠ | AY686864 Civets SARS          |
| * | KC869678 Bats MERS            |
| ⊞ | KY417150 Bats SARS            |
| ⊞ | MN996532 Bats SARS-CoV-2      |
| ⊞ | MT040336 Pangolins SARS-CoV-2 |
| ⊞ | NC_004718 Human SARS          |
| ⊞ | NC_038294 Human MERS          |
| ⊞ | NC_039207 Hedgehogs MERS      |
| ■ | NC_045512 Human SARS-CoV-2    |



Accession | Host | Virus

AY696864|Civets|SARS  
 KC869678|Bats|MERs  
 KY417150|Bats|SARS  
 MN996532|Bats|SARS-CoV-2  
 MT040336|Pangolins|SARS-CoV-2  
 NC\_004718|Human|SARS  
 NC\_038294|Human|MERs  
 NC\_039207|Hedgehogs|MERs  
 NC\_045512|Human|SARS-CoV-2



**A****B**